Multiscale monsoon variability during the last two climatic cycles revealed by spectral signals in Chinese loess and speleothem records

Y. Li[1], N. Su[2,3], L. Liang[1], L. Ma[1], Y. Yan[1], and Y. Sun[1]

[1]State Key Laboratory of Loess and Quaternary Geology, Institute of Earth Environment, Chinese Academy of Sciences, Xi'an, Shaanxi 710061, China

[2]College of Science, Technology and Engineering, James Cook University, Cairns, Queensland 4870, Australia

[3]School of Mathematics and System Science, Shenyang Normal University, Shenyang, Liaoning 110034, China

Correspondence to: Y. Li (liying@ieecas.cn) and Y. Sun (sunyb@ieecas.cn)

The authors greatly appreciate the crucial remarks made by the referees and the editor

---

Cpd-10-C2226-2015

1. Grain-size data have been widely used as a proxy for changes in winter monsoon strength in paleoclimatic studies of the Chinese Loess Plateau. A lot of sections of grain-size data with high-resolution and sufficient time length have been published, including cited and non-cited in the manuscript. A comparison with other grain-size data from high sedimentation rate and weak pedogenesis loess-paleosol sequences in this region is useful to test local or regional significance of the Gulang section. In particular, the authors should check if the millennial-scale events shown in Fig.6 could be validated in other loess sections? I suggest drawing a figure to show the nature of replication within the dating uncertainty.

Reply: In lines 6-9, page 5, and lines 18-21, page 11, we compared our Gulang mean grain size with a 249-kyr grain-size stack by Yang and Ding (2014), which includes grain size results of eight loess sections in the northern and western Chinese Loess Plateau, to check the repeatability and verify the regional significance of Gulang. Our grain size data show significant glacial-interglacial fluctuations and well-aligned rapid climatic oscillations similar to the grain size stack over the last two glacial cycles.

2. The composite speleothem data appeared in Fig.2 are problematic. The data sourced from the two references (Wang et al, 2008, Cheng et al, 2009) unlikely produce this figure. I guess that the authors subjectively selected other cave data (for example, a set of the penultmate glacial data published in Cheng et al, Geology, 2006) to replace some intervals of the cited data in the last two climate cycles. Please give an explanation for this replacement.

Reply: In lines 12-15, page 5, we clarified how to generate the composite speleothem

data. The $\delta^{18}O$ time series over the last two glacial cycles are from Sanbao/Hulu caves (0-224kyr, Wang et al., 2008) and Sanbao cave (224-260 kyr, Cheng et al., 2009). As Wang et al did, we plotted Hulu $\delta^{18}O$ 1.6‰ more negative than Sanbao cave values.

3. A total of 25 D/O events in the NGRIP ice records during the last glacial period are also seen in the Chinese speleothem records (Wang et al, 2008). However, I could not find additional 3 DO events (numbered from 26 to 28 in Fig.6) in the raw speleothem records. I suspect that the decomposing approach would produce illusive/noise signal such as the DO 26-28.

Reply: For comparison with rapid climate changes recorded in speleothem (Wang et al., 2008), we interpolate the raw grain size and the speleothem $\delta^{18}O$ data at 0.2 kyr resolution. The high frequency components were decomposed using Empirical Mode Decomposition (EMD) approach rather than filtering method in the revised manuscript. The EMD method extracts energy associated with intrinsic time scales in nonlinear fluctuations, and iteratively decomposes the raw complex signal into a series of elementary intrinsic model function (IMF) components, avoiding the probability of producing noise signals.

In Fig. 7, we marked millennial-events of the speleothem $\delta^{18}O$ record based on Wang et al. (2008), and identified well-aligned DO events between loess particle and speleothem $\delta^{18}O$ records over the last two glacial cycles. (lines 8-18, page 11)

4. The variances of 11 and 16% are too precise to be accepted due to more or less noise added to the climatic signal in the loess and speleothem records. The noise arises from either analytical errors or differences in amplitude of millennial-scale events between the same archives. For example, Fig. 2 shows many differences at millennial-scale changes from the data published in Nature (Wang et al, 2008).

Reply: In lines 6-8 and 15-16, page 8, we re-calculated the variances and

uncertainties of millennial-scale signals for both Gulang MGS and speleothem $\delta^{18}O$ records, which are 11 % and 17 %, respectively. We admit that the contributions of millennial components are not dominant in both records; however, they truly exist without noises since the variances cannot be changed by simply interpolation and decomposition using EMD method.

The validity of the millennial-scale fluctuations of Gulang MGS record is also supported by the good correlation between original and decomposed millennial component (Fig. R1) with similar amplitudes and numbers of evident events.

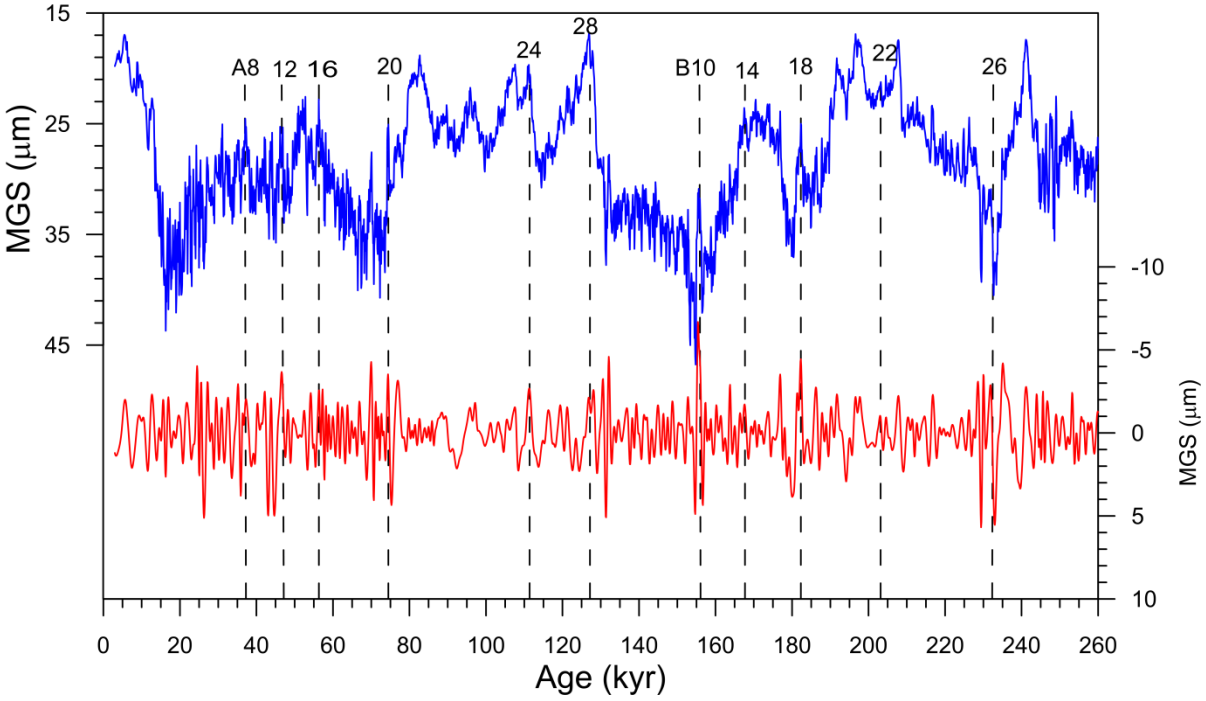

Figure R1. Comparison of millennial-scale component (red) with the raw data (blue) of Gulang MGS record. Dashed lines and numbers indicate some interstadials in the Chinese loess.

5. The author should give more detailed explanation for the tie-points in Fig.2. We know that the SPECMAP age model shows 3-5 thousand years younger than the speleothem records at the last three ice terminations.

Reply: In lines 4-6, page 5, we mentioned that a detailed description of Gulang chronology construction has already been published (Sun et al., 2015). In fact, we used optically stimulated luminescence ages for the last 60kyr (see Sun et al., 2012).

For the lower part, the Gulang MGS series is compared with benthic $\delta^{18}O$ record (Lisiecki and Raymo, 2005)，as it is well accepted that the East Asian winter monsoon variability was dynamically dominated by changes in global ice volume over the last two glacial cycles. 7 tie-points are selected by matching rapid changes of MGS and benthic $\delta^{18}O$ records during the major climatic boundaries for the interval of 260-60 kyr.

6. I wonder why Li et al have not described stratigraphy of the Gulang section (depth, loess-paleosol units). If published elsewhere, please cite it. It seems that parts of the data used in this manuscript have been already published in Catena (2011). However, I do not see the cited reference.

Reply: In lines 2-9, page 5, we clarified that grain size data of the upper 20 m were from a 20-m pit near Gulang, which has been published in Nature Geoscience (Sun et al., 2012), and grain size of the lower part spanning the last two glacial cycles was used for chronological reconstruction in another paper (Sun et al., 2015). However, in these two papers, multiscale variability of the MGS was not in-depth investigated. Unlike previous loess and speleothem papers, we decomposed multiscale variability recorded in these two proxies in order to evaluate their relative contributions, similarity and discrepancies.

Cpd-10-C2235-2015

1. *Though this study presented new high resolution loess grain size record over the past 260 kyr, there are no new and innovative discoveries in the physical mechanism of the past Asian monsoon variability*

Reply: East Asian monsoon (EAM) changes indeed have been extensively studied at various timescales using loess grain size and speleothem $\delta^{18}O$, and potential

dynamical drivers of EAM are well accepted including global ice volume and solar radiation at orbital timescale and high-latitude northern hemisphere climate on millennial timescale. Our results coincide with earlier finding in terms of EAM variability and mechanisms. However, apart from linking EAM signals to plausible driving forces, the main objectives of our studies are twofold. We clearly clarified our motivations in lines 10-14, page 4. First, we tried to evaluate the relative contributions of orbital and millennial signals in these two widely accepted monsoon proxies using spectral analysis and decomposing approaches. Second, we want to emphasize the glacial-interglacial discrepancy and millennial similarity between loess and speleothem records by comparison of the decomposed components of these two proxies. Our results confirmed that the extracted millennial-scale climatic events are almost identical in these two archives, which is very important for further evaluating the coupling between millennial-scale winter and summer monsoon variability.

2. They demonstrated that Asian speleothem $\delta^{18}O$ records are not a valid proxy for summer monsoon intensity only at the orbital timescale but rather reflect annual variations in hydrologic processes and circulation regime over a large part of the Indo-Asian region. Thus, the spectral analyses on the loess grain size record and the speleothem $\delta^{18}O$ record, more like a purified mathematical game, cannot distinguish the differences in the responses of the cyclic variations between the East Asian winter and summer monsoons to the orbital and internal forcings.

Reply: In lines 17-29, page 5, we demonstrated that Asian speleothem $\delta^{18}O$ may have different palaeoclimatic implications at various timescales, and thus the correlation between speleothem $\delta^{18}O$ record and monsoon is debatable. Fully investigation of the implication of speleothem $\delta^{18}O$ needs more proxy-to-proxy and proxy-to-model comparisons. Recent work by Liu et al (2014) suggests that Chinese speleothem $\delta^{18}O$ can be regarded as a monsoon proxy to reflect the southerly wind intensity rather than the precipitation change. As presented in our work, only multiscale variability were decomposed for this arguable monsoon proxy, the

discrepancy and similarity of different-scale variability compared with loess particle size record can provide more insights into the regional disparity and behind mechanisms. Based on our spectral and decomposed results, we can distinguish varied sensitivity of loess MGS and speleothem $\delta^{18}O$ records to glacial and orbital forcing; however, the well-aligned MGS and speleothem $\delta^{18}O$ fluctuations on the millennial scale do indicate that they likely share a common driving force.

3. The authors detected significant 100 kyr cycles in the 260-kyr long loess grain size record. Though the 100 kyr cycle exceeds the 80% significance level in mathematics, the significance of the 100 kyr cycle is questionable because the total length of the record is only 260 kyr, about two and half 100 kyr cycles, which is far beyond the limit of the statistical samples.

Reply: From a statistical perspective, the 260-kyr records are short to distinguish the 100 kyr periodicity. However, the 100-kyr glacial cycles can be evidenced by glacial-interglacial amplitude contrast. To confirm whether the 100-kyr cycle are robustly existed in loess grain size time series, in contrast to the dominant precessional cycles in speleothem record, we compared the 500 kyr MGS (Sun et al., 2006) and Hulu/Sanbao speleothem $\delta^{18}O$ records (Cheng et al., 2012) (Fig.R2). Spectral results of these two time series exhibit different peaks (Fig. R2), with a strong 100-kyr cycle at the Jingyuan MGS spectrum and a dominant 23-kyr period in the speleothem $\delta^{18}O$ spectrum. Jingyuan MGS record shows obvious glacial and interglacial differences, which confirms the 100 kyr period. The main periodicities detected from the 500 kyr loess and speleothem spectrum are quite similar to those from our current 260 kyr records, which further validates the reliability of our spectral results.

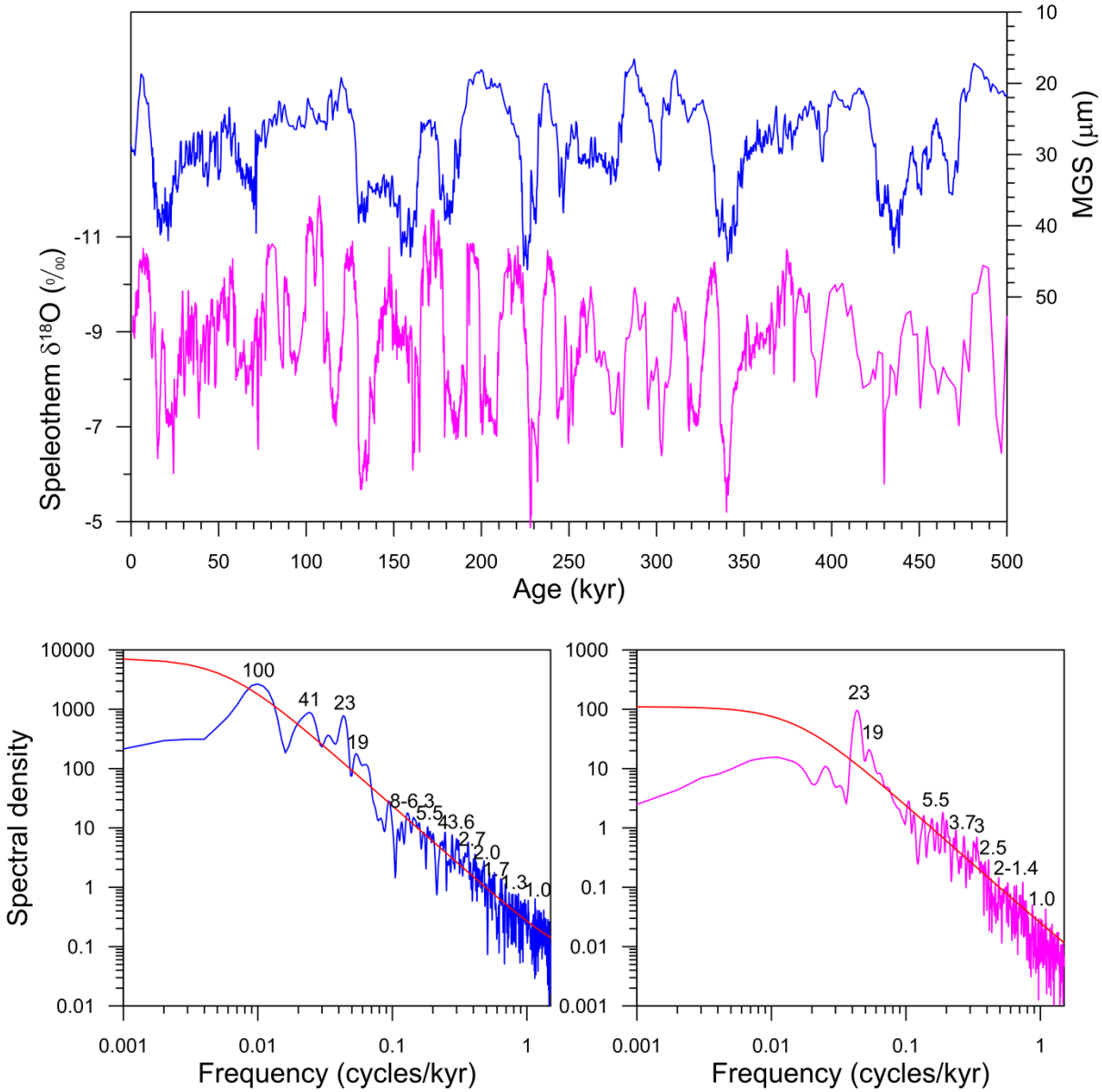

Figure R2. Original data (above) and spectral results (below) of Jingyuan MGS (blue; Sun et al., 2006) and Hulu/Sanbao speleothem $\delta^{18}O$ (purple; Cheng et al, 2012) records. The red lines represent the 90% confidence levels. Black numbers are identified periodicities.

Cpd-10-C2400-2015

1. The authors should confirm the results shown in Fig. 3, by applying at least another spectral technique not based on Fourier method. I suggest to use the Singular Spectrum Analysis (SSA, toolkit available online), which is well suited also for series affected by a high-noise level. SSA required equally-spaced data and therefore an interpolation is required.

Reply: In lines 2-5 and 19-21, page 7, we performed both Redfit and MTM (implemented in the SSA toolkit) methods on the loess grain size records, and found that the spectrum by these two approaches are highly comparable, confirming the reliability of Redfit spectral results.

2. Regarding the reconstruction of the variability components (Fig. 4, 5 and 6), the choice of the boundaries of the frequency bands C1, C2, : : :, C5 is somewhat arbitrary and the shape of the components reconstructed in Fig. 4 can depend on this choice. The arbitrariness in the choice of frequency bands can be overcome by extracting the components using SSA. A Monte Carlo test (more specific in respect to that corresponding to the red curves of Fig.3) is associated with SSA. By applying it, discrimination among the many components identified as significant in the C4 and C5 bands, should be possible.

Reply: In lines 14-20, page 6, we adopted Empirical Mode Decomposition (EMD) in the revised manuscript to extract the "intrinsic mode functions" (IMF) of Gulang MGS data and to further demonstrate the multi-scale features of East Asian monsoon variability. Since the EMD method is based on the local characteristic time scale of the data, can avoid the arbitrariness in the choice of frequency band.

3. It is not clear if the variances of the components in Fig. 4 are a percentage of the two raw series total variance. If the case, the corresponding components of the two series may contain different noise levels, thus distorting the comparison.

Reply: Yes, the variances are calculated on the raw time series. Noises of these two records were from the analytical errors, which are about 2% and 0.1% for the loess mean grain size and speleothem $\delta^{18}O$, respectively. However, the variances of orbital-to-millennial components are significantly higher than the analytical errors, and thus can be used for proxy-to-proxy comparison and further addressing different sensitivity of loess and speleothem proxies to orbital and glacial forcing.

4. *Please clarify if the loess measurements presented here are totally or partially new.*

Reply: In lines 2-9, page 5, we clarified that grain size data of the upper 20 m were from a 20-m pit near Gulang, which has been published in Nature Geoscience (Sun et

al., 2012), and grain size of the lower part spanning the last two glacial cycles was used for chronological reconstruction in another paper (Sun et al., 2015). However, in these two papers, multiscale variability of the MGS was not in-depth investigated. Unlike previous loess and speleothem papers, we firstly decompose multiscale variability recorded in these two proxies, in order to evaluate their relative contributions, similarity and discrepancies as well.

5. *I suggest to put in more evidence the new results presented in this work in respect to those previously obtained. I suggest to add a section briefly explaining the spectral methods used, the Monte Carlo procedure used to calculate the red curves in Fig. 3 and the applied filtering approach.*

Reply: We aware that East Asian monsoon variability and dynamics indeed have been extensively studied at various timescales using loess grain size and speleothem $\delta^{18}O$. Unlike previous works, the main objectives of our studies are twofold which is emphasized in lines 10-14, page 4. First, we tried to evaluate the relative contributions of orbital and millennial signals in these two widely accepted monsoon proxies using spectral analysis and decomposing approaches. Second, we want to emphasize the glacial-interglacial discrepancy and millennial similarity between loess and speleothem records by comparison of the decomposed components of these two proxies. Our results confirmed that the extracted millennial-scale climatic events are almost identical in these two archives, which is very important of further evaluating the coupling between millennial-scale winter and summer monsoon variability.

In addition, we performed different spectral (MTM and Redfit) and decomposing (EMD) methods with detailed descriptions (lines1-20, page 6) to detect the multiscale EAM variability.

Cpd-10-C2403-2015

1. Some references to important previous works are missing, a more detailed state of the art is requested and a comparison with other similar records should be provided.

Reply: In the revised version, we reviewed several more important works about East Asian monsoon variability and dynamics at various timescales using loess grain size and speleothem $\delta^{18}O$ records. We clarified the main objectives of our work (lines 10-14, page 4) to evaluate the relative contributions of orbital and millennial signals in loess grain size and speleothem $\delta^{18}O$ proxies. Unlike previous work, our result emphasized the glacial-interglacial differences and millennial similarity between loess and speleothem records. Meanwhile, we compared our grain size variations with similar records, e.g., median size variation of 249-kyr grain-size stack by Yang and Ding (2014). Moreover, we cited the 500-kyr mean grain size of Jingyuan section (Sun et al., 2006), and 500-kyr Hulu/Sanbao $\delta^{18}O$ (Cheng et al., 2012) records to validate our spectral and decomposing results.

2. The interpretation of the spectral analysis is questionable and, at least, additional analyses must be provided to support the conclusions.

Reply: We performed MTM, Redfit and EMD methods to confirm our spectral and decomposed components results. Detail results can be seen in the responses to the Cpd-10-C2400-2015.

References

Cheng, H., Edwards, R. L., Broecker, W. S., Denton, G. H., Kong, X., Wang, Y., Zhang, R., and Wang, X.: Ice age terminations, *Science*, 326, 248–252, 2009.

Cheng, H., Zhang, P. Z., Spötl, C., Edwards, R. L., Cai, Y. J., Zhang, D. Z., Sang, W. C., Tan, M., An, Z. S., 2012. The climatic cyclicity in semiarid-arid central Asia over the past 500,000 years. *Geophys Res Lett*, **39**, L01705. Doi:10.1029/2011GL050202.

Lisiecki, L. E. and Raymo, M. E.: A Pliocene-Pleistocene stack of 57 globally distributed benthic $\delta^{18}O$ records, *Paleoceanography*, 20, PA1003, doi:10.1029/2004PA001071, 2005.

Liu, Z. Y., Wen, X. Y., Brady, E. C., Otto-Bliesner, B., Yu, G., Lu, H. Y., Cheng, H., Wang, Y. J., Zheng, W. P., Ding, Y. H., Edwards, R. L., Cheng, J., Liu, W., Yang, H., 2014. Chinese cave records and the East Asia Summer Monsoon. *Quaternary Sci Rev*, **83**: 115-128.

Sun, Y. B., Clemens, S. C., Liu, Q. S., Ji, J. F., Tada, R., 2006. East Asian monsoon variability over the last seven glacial cycles recorded by a loess sequence from the northwestern Chinese Loess Plateau. *Geochem Geophys Geosyst*, **7**, Q12Q02. Doi:10.1029/2006GC001287.

Sun, Y., Clemens, S. C., Morrill, C., Lin, X.,Wang, X., and An, Z.: Influence of Atlantic meridional overturning circulation on the East Asian winter monsoon, *Nat Geosci*, 5, 46–49, 2012.

Sun, Y., Kutzbach, J., An, Z., Clemens, S., Liu, Z., Liu, W., Liu, X., Shi, Z., Zheng, W., Liang, L., Yan, Y., and Li, Y.: Astronomical and glacial forcing of East Asian summer monsoon variability, *Quaternary Sci. Rev.*, 115, 132-142, 2015.

Wang, Y., Cheng, H., Edwards, R. L., Kong, X., Shao, X., Chen, S., Wu, J., Jiang, X., Wang, X., and An, Z.: Millennial and orbital-scale changes in the East Asian monsoon over the past 224,000 years, *Nature*, 451, 1090–1093, 2008.

Wu, G., Pan, B., Guan, Q., and Xia, D.: Terminations and their correlation with solar insolation in the Northern Hemisphere: a record from a loess section in Northwest China, *Palaeogeogr. Palaeocl., Palaeoecol.* 216, 267-277, 2005.

Yang, S. and Ding, Z.: A 249 kyr stack of eight loess grain size records from northern China documenting millennial-scale climate variability, *Geochem. Geophy. Geosy*., 15, 798–814, 2014.

A list of relevant changes

The authors are sorry for not being able to provide a list of relevant changes since this manuscript experienced a thorough revision in terms of grain size chronology construction, spectral and decomposing methods and results.

Abstract

The East Asian Monsoon exhibits a significant variability on timescales ranging from tectonic to centennial as inferred from loess, speleothem and marine records. However, the relative contributions and plausible driving forces of the monsoon variability at different timescales remain controversial. Here, we spectrally explore time series of loess grain size and speleothem $\delta^{18}O$ records and decompose the two proxies into intrinsic components using Empirical Mode Decomposition method. Spectral results of these two proxies display clear glacial-and-orbital periodicities corresponding to ice-volume and orbital cycles, and evident millennial signals which are in pace with Heinrich rhythm and DO cycles. Six intrinsic components are parsed out from loess grain size and speleothem $\delta^{18}O$ records, respectively, and combined signals are correlated further with possible driving factors including the ice volume, insolation and North Atlantic cooling. The relative contributions of six components differ significantly between loess grain size and speleothem $\delta^{18}O$ records. Coexistence of glacial and orbital components in the loess grain size implies that both ice volume and insolation have distinctive impacts on the winter monsoon variability, in contrast to the predominant precessional impact on the speleothem $\delta^{18}O$ variability. Moreover, the millennial components are evident with variances of 10 % and 17 % in the loess grain size and speleothem $\delta^{18}O$ records, respectively. A comparison of the millennial-scale signals of these two proxies reveals that abrupt changes in the winter and summer monsoons over the last 260 kyr share common features and similar driving forces linked to high-latitude Northern Hemisphere climate.

1 Introduction

The East Asian Monsoon (EAM), as a significant part of Asian monsoon circulation, plays an important role in driving the palaeoenvironmental changes in East Asia (An, 2000). The EAM fluctuations can be quantified at different time intervals ranging from thousands of years to intraseasonal periodicities, and the primary driving force of the monsoon variability on each timescale is not unique (An et al., 2015). Multiscale monsoon variability has been inferred from numerous proxies generated from deep-sea sediments (e.g., Wang et al., 1999; Wang et al., 2005), eolian deposits (e.g., An, 2000, Sun et al., 2012), and speleothem records

(e.g., Wang et al., 2001, 2008), which provide valuable insights into the changing processes and potential driving forces of the EAM variability. In particular, Chinese loess has been investigated intensively as a direct and complete preserver of the EAM changes, with great efforts on deciphering on the EAM variability on both orbital and millennial scales (e.g., An et al., 1990; Ding et al., 1994, 2002; Porter and An, 1995; Guo et al., 1996; Chen et al., 1997; Liu and Ding, 1998; Liu et al., 1999; An, 2000; Chen et al., 2006).

On the orbital timescale, the EAM variation recorded by Chinese loess-paleosol sequences was characterized by an alternation between the dry-cold winter monsoon and the wet-warm summer monsoon (Liu and Ding, 1998; An, 2000). A strong 100 kyr periodicity was detected in the Chinese loess particle size record, implying an important impact of glacial boundary conditions on the EAM evolution (Ding et al., 1995). Obliquity and precession signals were also clear in loess based proxies (Liu et al., 1999; Ding et al., 2002; Sun et al., 2006). Apart from these dominant periodicities, some harmonic periodicities related to orbital parameters were also found in the EAM records, such as the ~75, ~55, and ~30 kyr spectral peaks (Lu et al., 2003; Sun et al., 2006; Yang et al., 2011). In contrast, absolute-dated speleothem $\delta^{18}O$ records revealed an evident 23 kyr cycle, implying a dominant role of summer insolation in driving the summer monsoon variability (Wang et al., 2008; Cheng et al., 2009). Different variances of obliquity and precession signals in monsoonal proxies suggest that the responses of the winter and summer monsoons to the orbital forcing were dissimilar (Shi et al., 2011). The various patterns of orbital-scale monsoon fluctuations between the loess proxies and speleothem $\delta^{18}O$ records likely reflected the sensitivity of various archives and proxies to the EAM variability (Clemens et al., 2010; Cheng et al., 2012; Sun et al., 2015; Cai et al., 2015).

At the millennial timescale, the rapid monsoon oscillations inferred from Chinese loess were not only persistent during the last two glacial cycles (Porter and An, 1995; Guo et al., 1996; An and Porter, 1997; Chen et al., 1997; Ding et al., 1999; Sun et al., 2010; Yang and Ding, 2014), and were also evident during early glacial extreme climatic conditions (Lu et al., 1999). The millennial-scale monsoon variability during the last glacial period was strongly coupled to climate changes recorded in Greenland ice-core and North Atlantic sediments, indicating a dynamic connection between the EAM variability and the high-latitude Northern

Hemisphere climate (Porter and An, 1995; Guo et al., 1996; Chen et al., 1997; Fang et al., 1999). Recently, a combination of proxies from Chinese loess, speleothem, and Greenland ice-core with modeling results indicated that the Atlantic meridional overturning circulation might have played an important role in driving the rapid monsoon changes in East Asia (Sun et al., 2012).

Though previous studies have revealed that past EAM variabilities principally comprise a mixture of forcing signals from ice volume, solar radiation, and North Atlantic climate, the relative contributions of glacial, orbital and millennial forcing to the EAM variability remain unclear. In this study, we conducted a comprehensive investigation of multiscale EAM variability over the last 260 kyr, by analyzing mean grain size (MGS) record from a Gulang loess sequence (a proxy indicator of the East Asian winter monsoon intensity) and speleothem $\delta^{18}O$ record of Hulu and Sanbao caves (a debatable indicator of the summer monsoon intensity). These two representative time series were decomposed to obtain intrinsic components of the climatic signals, which were further compared with potential driving factors. Our objectives are to evaluate the relative contributions of glacial–interglacial to millennial signals registered in these two widely employed monsoon proxies, and to emphasize the glacial-interglacial discrepancy and millennial similarity between loess and speleothem records.

2 Data and methods

The data for the loess sequence was collected at a section in Gulang, Gansu Province, China (37.49 ºN, 102.88 ºE, 2400 ma.s.l.), which is situated in the northwestern part of the Chinese Loess Plateau. It is about 10 km to the southwest margin of the Tengger desert (Fig. 1). In this region, the average annual precipitation and temperature over the last 20 years are 350 mm and 5.7 ℃, respectively. About 70 m loess was accumulated at Gulang during the last two climate cycles. High sedimentation rate and weak pedogenesis in this region make the Gulang loess sequence very sensitive to orbital and millennial monsoon changes (Sun et al., 2012, 2015). The samples used in this study were collected at 2cm intervals, corresponding to

50–100 yr resolution for the loess-paleosol sequence. Before the measurements of grain sizes, all samples were firstly pretreated by removing carbonate and organic matter using 30% HCL and 10% H_2O_2, respectively, and then dispersed under ultrasonification in 10ml 10% $(NaPO_3)_6$ solution. A Malvern 2000 laser instrument was employed for determining the grain size distribution which has an analytical error of < 2% as revealed by replicate analyses. The grain size data of the upper 20 m were from a 20-m pit near Gulang (Sun et al., 2012), and the lower part spanning the last two glacial cycles was from another 50-m section. Mean grain size data of the composite 70-m section have been employed for a chronological reconstruction (for a detailed description, see Sun et al., 2015). The Gulang chronology was evaluated by comparison with a 249-kyr grain size stack (CHILOMOS) record in the northern Loess Plateau (Yang and Ding, 2014) (Fig.2); the good matches between these two records imply a high reliability of our Gulang age construction. Unlike previous studies (Sun et al., 2012, 2015), we performed spectral and decomposing analysis on the mean grain size time series in order to decipher multiscale variability and dynamics of the winter monsoon.

The absolute-dated speleothem $\delta^{18}O$ records from Sanbao/Hulu caves (0-224 kyr, Wang et al., 2008) and the Sanbao cave (224-260 kyr, Cheng et al., 2009) (Fig. 1) were selected to infer summer monsoon variability spanning the last two glacial–interglacial cycles. Compatible with the analysis by Wang et al (2008), we plot the Hulu $\delta^{18}O$ data 1.6‰ more negative than that from the Sanbao cave (Fig. 2). Interpretation of the Chinese speleothem $\delta^{18}O$ records remains debatable as a direct indicator of summer monsoon intensity since various factors like seasonal changes in precipitation amount, moisture sources, and circulation patterns would influence the speleothem $\delta^{18}O$ composition (e.g., Yuan et al., 2004; Wang et al., 2001, 2008; Cheng et al., 2009; Clemens et al., 2010; Dayem et al., 2010; Pausata et al., 2011; Maher and Thompson, 2012; Caley et al., 2014). Nevertheless, high similarity between millennial events in Chinese speleothem and Greenland ice core revealed that speleothem $\delta^{18}O$ is a reliable indicator of seasonal monsoon change (Wang et al., 2001; Clemens et al., 2010). More recently, a model-data comparison suggested that Chinese speleothem $\delta^{18}O$ can be regarded as a monsoon proxy to reflect the southerly wind intensity rather than the precipitation change (Liu et al, 2014). Thus, spectral and decomposed results of the

composite speleothem $\delta^{18}O$ record time series were used in this study to address multiscale variability and dynamics of the summer monsoon.

To detect the presence of glacial-to-millennial periodicities, we performed spectral analysis on the 260 kyr records of Gulang MGS and speleothem $\delta^{18}O$ using both of Multitaper (MTM, implemented in the SSA toolkit, Vautard et al., 1992) (http://www.atmos.ucla.edu/tcd/ssa/) and REDFIT (Schulz and Mudelsee, 2002) methods, which are related to Empirical Orthogonal Function and Lomb–Scargle Fourier transform, respectively. MTM method has the advantages of being suitable for series affected by high-noise levels, and incorporating significance test which is not proportional to the power of spectrum, confirming the detection of low-amplitude periodicities (Lu et al., 1999), while the REDFIT program estimates the first-order autoregressive (AR1) parameter from unevenly space time series without interpolation, which avoids a too "red" spectrum (Schulz and Stattegger, 1997). The similar spectral periodicities derived from both REDFIT and MTM methods were regarded as dominant frequencies at glacial-to-millennial bands.

The decomposed components of loess MGS and speleothem $\delta^{18}O$ records were parsed out using the technique of Empirical Mode Decomposition (EMD) (Huang et al., 1998). EMD directly extracts energy which is associated with intrinsic time scales in nonlinear fluctuations, and iteratively decomposes the raw complex signal with several characteristic time scales coexisting into a series of elementary intrinsic model function (IMF) components, avoiding any arbitrariness in the choices of frequency bands in this multiscale study. The EMD method has been widely employed over various palaeoclimate database, such as ice-cover (Gloersen and Huang, 2003), North Atlantic oscillation (Hu and Wu, 2004), solar insolation (Lin and Wang, 2006), and temperature under global warming (Molla et al., 2006). However, the application of EMD method on the loess record remains poorly investigated with some understanding of decomposed components at glacial-and-orbital scale (Yang et al., 2001, 2008). In this study, we applied EMD on high-resolution loess and speleothem data records to quantify the relative contributions of both orbital and millennial components.

3 Multiscale monsoon variability

The highly comparable spectral results between REDFIT and MTM methods show that apparent periods identified in the MGS spectrum are at ~100, ~41, ~23, ~15, ~7, ~5, and ~3-1 kyr over the 80 % and 90 % confidence levels, respectively, for REDFIT and MTM methods (Fig. 3). It is shown that the potential forcing of the glacial–interglacial and orbital EAM variability is part of the external (e.g., the orbital-induced summer insolation, An, 1991; Wang et al., 2008) and the internal factors (e.g., the changes in the ice volume and CO_2 concentrations, Ding et al., 1995; Lu et al., 2013; Sun et al., 2015). The coexistence of the ~100, ~41, and ~23 kyr periods in the Gulang MGS record confirms the dynamic linkage of the winter monsoon variability to glacial and orbital forcing. Based on the spectral results, many millennial frequencies are detected, which can be mainly divided into two groups of ~7-5 and ~3-1 kyr, which, possibly correspond, respectively, to the Heinrich (~6 kyr) rhythm and the Dansgaard–Oeschger (DO, ~1.5 kyr) cycles recorded in the North Atlantic sediments and Greenland ice core (Bond et al., 1993; Dansgaard et al., 1993; Heinrich, 1988). Taking into account the sampling resolution and surface mixing effect at Gulang, the residual component (< 1 kyr) might contain both centennial and noisy signals, which is excluded for further discussion in this study.

Compared to the MGS spectral results, the speleothem $\delta^{18}O$ spectrum shares similar peaks at the precession (~23 kyr) and millennial bands (~5, ~3, ~2.4, ~2, ~1.5, ~1.3, and ~1 kyr), but is lack of distinct peaks at ~100 kyr and ~41 kyr (Fig. 3). Notably, precession peaks at ~23 and ~19 kyr are more dominant in the speleothem $\delta^{18}O$ than in the loess MGS record. Moreover, the speleothem spectrum shows a peak over the 80 % and 90 % confidence levels in REDFIT and MTM spectrum, respectively, centered at ~10 kyr frequency, which is, approximately, related to the semi-precession frequency.

The different oscillation patterns composing loess MGS and speleothem $\delta^{18}O$ time series are separated out using EMD method as presented in Fig. 4 and Fig. 5, respectively, together with dominant periods as shown. Six IMFs are generated for the Gulang MGS data on glacial-to-millennial timescale. The periodicities in IMF3 span 19-10 kyr likely correspond to the second precessional cycle. The variability of Gulang MGS is dominated by the lowest frequency signal with variances of 38 % (IMF6). Two orbital components (IMF5 and IMF4)

are linked to obliquity and precession, contributing equally 23 % to the total variance. The variances of two millennial components (IMF2 and IMF1) are very close (5 %) in the Gulang MGS record. Similarly, six IMFs are decomposed for the speleothem $\delta^{18}O$ record on frequencies lower than 1 kyr, and all the glacial-to-orbital periodicities correspond to Milankovitch parameters. Compared with decomposed results of Gulang MGS record, glacial (IMF6) and obliquity (IMF5) components are not clear in the speleothem $\delta^{18}O$ record with variances of 11 % and 8 %, respectively. The precession component (IMF4), however, is the most dominant signal among the six components, accounting for 56 % of the variance. A notable semi-precession component (IMF3) contributes 8 % of the total variance, and two millennial components are also evident with variances of 12 % and 5 %, respectively.

4 Dynamics of multiscale EAM variability

4.1 Glacial and orbital forcing of the EAM variability

We combine IMF3, 4, 5, and 6 of Gulang MGS and speleothem $\delta^{18}O$ records as the low-frequency signals (>10 kyr) to reveal the glacial-and-orbital scale variations of the winter and summer monsoon, respectively. The glacial-and-orbital variations of the loess and speleothem records represent the total variances of ~90 % and ~83 %, respectively. The low-frequency signals of the loess MGS and speleothem $\delta^{18}O$ records are compared with changes in the ice volume and solar insolation at 65 ℃N (Berger, 1978) to ascertain plausible impacts of glacial and orbital factors on the EAM variability (Fig. 6).

The low-frequency component of the Gulang MGS record is well correlated with global ice volume change inferred from the benthic $\delta^{18}O$ record (Lisiecki and Raymo, 2005), reinforcing the strong coupling between the winter monsoon variation and ice-volume changes (Ding et al., 1995). Besides the glacial–interglacial contrast, fine MGS signals at the precessional scale seem more distinctive than those in the benthic $\delta^{18}O$ stack. For example, the remarkable peaks in the MGS around 50, 85, 110, and 170 kyr have no counterpoints in the benthic $\delta^{18}O$ record. By comparing MGS data with the summer insolation record, the overall ~20 kyr periodicity is damped but still visible during both glacial and interglacial periods, except for insolation

maxima around 150 and 220 kyr (Fig. 6). The coexistence of the glacial and orbital cycles in loess MGS indicates that both the ice volume and solar insolation have affected the winter monsoon variability, and their relative contributions are 38 % and 52 %, respectively, as estimated from variances of the glacial (IMF6) and orbital (IMF5-3) components.

The speleothem $\delta^{18}O$ record varies quite synchronously with the July insolation, characterized by a dominant precession frequency (Fig. 6). This in-phase change is thought to support a dominant role of summer insolation in the Northern Hemisphere in driving the summer monsoon variability at the precession period (Wang et al., 2008), given that the palaeoclimatic interpretation of the speleothem $\delta^{18}O$ is quite controversial (Wang et al., 2001, 2008; Yuan et al., 2004; Hu et al., 2008; Cheng et al., 2009; Peterse et al., 2011).

The different contributions of glacial and orbital variability in the loess MGS and speleothem $\delta^{18}O$ records indicate that the driving forces associated with these two proxies are different. The loess grain size is directly related to the northwesterly wind intensity, reflecting that atmospheric surface process is linked to the Siberian-Mongolian High (Porter and An, 1995). The speleothem $\delta^{18}O$ might be influenced by multiple factors such as the isotopic depletion along the vapor transport path (Pausata et al., 2011), changes in $\delta^{18}O$ values of meteoric precipitation or the amount of summer monsoon precipitation (Wang et al., 2001, 2008; Cheng et al., 2009), and seasonality in the amount and isotopic composition of rainfall (Clemens et al., 2010; Dayem et al., 2010; Maher and Thompson, 2012).

It is quite clear that the EAM is formed by the thermal gradient between the Asian continent and the Pacific Ocean to the east and southeast (Halley, 1986; Xiao et al., 1995; Lestari and Iwasaki, 2006). In winter, due to a much larger heat capacity of water in the ocean than that on the land surface, a higher barometric pressure forms over the colder Asian continent with a lower pressure over the warmer ocean. This gradient is the driving force for the flow of cold and dry air out of Asia, consequently, the winter monsoon forms (Gao, 1962). On the glacial–interglacial timescale, the buildup of the northern high-latitude ice sheets during the glacial periods strengthens the barometric gradient which results in intense winter monsoons (Ding et al., 1995; Clark et al., 1999). The contemporaneous falling sea level and land-ocean pressure gradient further enhances winter monsoon circulation during glacial times (Xiao et al.,

1995). The other factor that influences the land-ocean differential thermal motion is the orbitally induced solar radiation changes. The precession-induced insolation changes can lead to regional land-ocean thermal gradients whilst obliquity-related insolation changes can result in meridional thermal gradients; both of which can substantially alter the evolution of the Siberian and Subtropical Highs and the EAM variations (Shi et al., 2011).

4.2 Impacts of high-latitude cooling on millennial EAM oscillations

The EAM variations are persistently punctuated by apparent millennial-scale monsoon events (Garidel-Thoron et al., 2001; Wang et al., 2001; Kelly et al., 2006). The millennial-scale events of the last glacial cycle were firstly identified in Greenland ice cores (Dansgaard et al., 1993; Meese et al., 1997). Subsequently, well-dated loess grain size and speleothem $\delta^{18}O$ records in China have been found to have apparent correspondences with rapid climate oscillations in the North Atlantic (Porter and An, 1995; Guo et al., 1996; Chen et al., 1997; Ding et al., 1998; Wang et al., 2001). The most striking evidence is the strong correlation between the loess grain size, speleothem $\delta^{18}O$ and Greenland ice core $\delta^{18}O$ records during the last glaciation (Ding et al., 1998; Wang et al., 2001; Sun et al., 2012). These abrupt changes have been extended into the past glacial–interglacial cycles from loess and speleothem records (Ding et al., 1999; Cheng et al., 2006, 2009; Wang et al., 2008; Yang and Ding, 2014) and from the North Atlantic sediments (McManus et al., 1999; Channell et al., 2012).

Here IMF1 and 2 components of the loess MGS and speleothem $\delta^{18}O$ records are combined to be considered as millennial-scale signals of the winter and summer monsoons, with variances of 10 % and 17 %, respectively. The combination of the two millennial signals of the loess MGS and speleothem $\delta^{18}O$ records are compared with the North Atlantic cooling events over the last two glacial cycles, to reveal the dynamic links of abrupt climate changes in East Asia and the North Atlantic (Fig. 7). The Younger Dryas (YD) and Heinrich Events (H_1-H_6) are well detected in loess and speleothem records around 12, 16, 24, 31, 39, 48, 55, and 60 kyr, respectively. Most of the millennial-scale events in the loess MGS and speleothem $\delta^{18}O$ records are well aligned with comparable amplitude and duration during the last two glacial cycles. However, some MGS valleys such as A17, A23, and B17-19 are not

well matched with the speleothem $\delta^{18}O$ minima, possibly due to uncertainties in the loess chronology. The comparable millennial scale events between grain size of Gulang and CHILOMOS stack (Yang and Ding, 2014) shows the nature of replication of Gulang MGS record within the dating uncertainty, confirming the persistent millennial-scale winter monsoon variability spanning the last two glacial cycles (Fig. 7).

The millennial-scale monsoon signals have been well compared with the cooling events recorded in the North Atlantic sediments, demonstrating a dynamic link between abrupt climate changes in East Asia and the North Atlantic. As identified in Chinese speleothem records, the magnitudes of abrupt climate events are identical between the last and the penultimate climatic cycles (Wang et al., 2008). However, the duration and amplitude of these millennial events seems quite different between the glacials and interglacials. The duration of millennial monsoon events is relatively shorter and the amplitude larger during glacial periods, suggesting a plausible glacial modulation on rapid climate changes (McManus et al., 1999; Wang et al., 2008). The potential driving mechanism for rapid EAM changes has been attributed to changing climate in the high-latitude Northern Hemisphere, e.g., the reduction of the North Atlantic deep water circulation triggered by fresh water inputs from melting icebergs (Broecker, 1994). The North Atlantic cooling can affect the zonal high pressure systems, including the Azores- Ural-Siberian-Mongolian high (Palmer and Sun, 1985; Rodwell et al., 1999; Yuan et al., 2004), which can further transmit the abrupt cooling effect into East Asia and result in significant EAM changes (Porter and An, 1995; Wang et al., 2001). Apart from the geological evidence, numerical modeling also suggests that the Atlantic meridional overturning circulation might affect abrupt oscillations of the EAM, while the westerly jet is the important conveyor introducing the North Atlantic signal into the EAM region (Miao et al., 2004; Zhang and Delworth, 2005; Jin et al., 2007; Sun et al., 2012).

5 Conclusions

The multiscale signals were spectrally detected and naturally decomposed from Chinese loess and speleothem records over the last two climatic cycles, permitting an evaluation of the relative contributions of glacial, orbital and millennial components in the EAM record.

Spectrum of Gulang MGS and speleothem $\delta^{18}O$ data show similar periodicities at glacial-to-orbital and millennial timescales, corresponding to the rhythms of changing ice-volume, orbitally induced insolation, and North Atlantic cooling (i.e., Heinrich rhythm and Dansgaard–Oeschger cycles), respectively. Amplitude variances of the decomposed components reveal significant glacial and orbital impacts on the loess grain size variation and a dominant precession forcing in the speleothem $\delta^{18}O$ variability. The millennial components are evident in the loess and speleothem proxies with variances of 10 % and 17 %, respectively. Two millennial IMFs were combined to recognize the synchronous nature of rapid changes of these two proxies. High similarity of millennial-scale monsoon events both in terms of the magnitudes and rhythms between the loess and speleothem proxies implies that the winter and summer monsoons share common millennial features and similar driving forces.

Acknowledgements

We thank J. Zhao, L. He, M. Zhao, and H. Wang for assistance in field sampling and lab measurements. Three anonymous reviewers and Dr. Loutre Marie-France are acknowledged for their insightful comments. This work was supported by funds from the National Basic Research Program of China (2013CB955904), the Chinese Academy of Sciences (KZZD-EW25 TZ-03), the National Science Foundation of China (41472163), and the State Key Laboratory of Loess and Quaternary Geology (SKLLQG1011).

References

An, Z. and Porter, S. C.: Millennial-scale climatic oscillations during the last interglaciation in central China, Geology, 25, 603–606, 1997.

An, Z., Liu, T., Lu, Y., Porter, S. C., Kukla, G., Wu, X., and Hua, Y.: The long-term paleomonsoon variation recorded by the loess-paleosol sequence in Central China, Quatern. Int., 7, 91–95, 1990.

An, Z., Wu, G., Li, J., Sun, Y., Liu, Y., Zhou, W., Cai, Y., Duan, A., Li, L., Mao, J., Cheng, H., Shi, Z., Tan, L., Yan, H., Ao, H., Chang, H., and Juan, F.: Global monsoon dynamics and climate change, Annu. Rev. Earth. Planet. Sci., 42, doi:10.1146/annurev-earth-060313-054623, 2015.

An, Z.: Magnetic susceptibility evidence of monsoon variation on the Loess Plateau of central China during the last 130,000 years, Quaternary Res., 36, 29–36, 1991.

An, Z.: The history and variability of the East Asian paleomonsoon climate, Quaternary Sci. Rev., 19, 171–187, 2000.

Berger, A.: Long-term variations of daily insolation and Quaternary climate changes, J. Atmos. Sci., 35, 2362-2367, 1978.

Bond, G., Broecker,W., Johnsen, S., McManus, J., Labeyrie, L., Jouzel, J., and Bonani, G.: Correlations between climate records from North Atlantic sediments and Greenland ice, Nature, 365, 143–147, 1993.

Broecker, W. S.: Massive iceberg discharges as triggers for global climate change, Nature, 372, 421–424, 1994.

Cai, Y., Fung, I. Y., Edwards, R. L., An, Z., Cheng, H., Lee, J. E., Tan, L., Shen, C. C., Wang, X., Day, J. A., Zhou, W. J., Kelly, M. J., and Chiang, J. C. H.: Variability of stalagmite-inferred Indian monsoon precipitation over the past 252,000 y, Proc. Natl. Acad. Sci. U. S. A., 112, 2954-2959, 2015.

Caley, T., Roche, D. M., and Renssen, H.: Orbital Asian summer monsoon dynamics revealed using an isotope-enabled global climate mode, Nat. Commun., 5,

doi:10.1038/ncomms6371, 2014.

Channell, J. E. T., Hodell, D. A., Romero, O., hillaire-Marcel, C., Vernal, A. D., Stoner, J. S., Mazaud, A., and Röhl, U.: A 750-kyr detrital-layer stratigraphy for the North Atlantic (IODP Sites U1302–U1303, Orphan Knoll, Labrador Sea), Earth Planet. Sc. Lett., 317–318, 218–230, 2012.

Chen, F., Bloemendal, J., Wang, J., Li, J., and Oldfield, F.: High-resolution multi-proxy climate records from Chinese loess: evidence for rapid climatic changes over the last 75 kyr, Palaeogeogr. Palaeocl., 130, 323–335, 1997.

Chen, J., Chen, Y., Liu, L., Ji, J., Balsam, W., Sun, Y., and Lu, H.: Zr/ Rb ratio in the Chinese loess sequences and its implication for changes in the East Asian winter monsoon strength, Geochim. Cosmochim. Ac., 70, 1471–1482, 2006.

Cheng, H., Edwards, R. L., Broecker, W. S., Denton, G. H., Kong, X., Wang, Y., Zhang, R., and Wang, X.: Ice age terminations, Science, 326, 248–252, 2009.

Cheng, H., Edwards, R. L., Kong, X., Ming, Y., Kelly, M. J., Wang, X., Gallup, C. D., and Liu, W.: A penultimate glacial monsoon record from Hulu Cave and two-phase glacial terminations, Geology, 34, 217–220, 2006.

Cheng, H., Zhang, P., Spötl, C., Edwards, R. L., Cai, Y., Zhang, D., and Sang, W.: The climate cyclicity in semiarid-arid central Asia over the past 500,000 years, Geophys. Res. Lett., 39, L01705, doi:10.1029/2011GL050202, 2012.

Clark, P. U., Alley, R. B., and Pollard, D.: Northern Hemisphere ice-sheet influences on global climate change, Science, 286, 1104–1111, 1999.

Clemens, S. C., Prell, W. L., and Sun, Y.: Orbital-scale timing and mechanisms driving Late Pleistocene Indo-Asian summer monsoons: reinterpreting cave speleothem $\delta^{18}O$, Paleoceanography, PA4207, doi:10.1029/2010PA001926, 2010.

Dansgaard, W., Johnsen, S. J., Clausen, H. B., Dahl-Jensen, D., Gundestrup, N. S., Hammer, C. U., Hvidberg, C. S., Ste_ensen, J. P., Sveinbjornsdottir, A. E., Jouzel, J., and Bond, G.: Evidence for general instability of past climate from a 250-kyr ice-core record, Nature, 364,

218–220, 1993.

Dayem, K. E., Molnar, P., Battisti, D. S., and Roe, G. H.: Lessons learned from oxygen isotopes in modern precipitation applied to interpretation of speleothem records of paleoclimate from eastern Asia, Earth Planet. Sc. Lett., 295, 219–230, 2010.

Ding, Z., Derbyshire, E., Yang, S., Yu, Z., Xiong, S., and Liu, T.: Stacked 2.6-Ma grain size record from the Chinese loess based on five sections and correlation with the deep-sea $\delta^{18}O$ record, Paleoceanography, 17, 5-1-5-21, 2002.

Ding, Z., Liu, T., Rutter, N. W., Yu, Z., Guo, Z., and Zhu, R.: Ice-Volume forcing of East Asian winter monsoon variations in the past 800,000 years, Quaternary Res., 44, 149–159, 1995.

Ding, Z., Ren, J., Yang, S., and Liu, T.: Climate instability during the penultimate glaciation: evidence from two high-resolution loess records, China, J. Geophys. Res., 104, 20123–20132, 1999.

Ding, Z., Rutter, N. W., Liu, T., Ren, J., Sun, J., and Xiong, S.: Correlation of Dansgaard–Oeschger cycles between Greenland ice and Chinese loess, Paleoclimates, 4, 281–291, 1998.

Ding, Z., Yu, Z., Rutter, N. W., and Liu, T.: Towards an orbital time scale for Chinese loess deposits, Quaternary Sci. Rev., 13, 39–70, 1994.

Fang, X., Pan, B., Guan, D., Li, J., Yugo, O., Hitoshi, F., and Keiichi, O.: A 60000-year loess-paleosol record of millennial-scale summer monsoon instability from Lanzhou, China, Chinese Sci. Bull., 44, 2264–2267, 1999.

Gao, Y.: On some problems of Asian monsoon, in: Some Questions About the East Asian Monsoon, edited by: Gao, Y., Science Press, Beijing, 1–49, 1962.

Garidel-Thoron, T. D., Beaufort, L., Linsley, B. K., and Dannenmann, S.: Millennial-scale dynamics of the East Asian winter monsoon during the last 200,000 years, Paleoceanography, 16, 491–502, 2001.

Gloersen, P. and Huang, N.: Comparison of interannual intrinsic modes in hemispheric ice covers and other geophysical parameters, IEEE Transactions in Geosciences and Remote

Sensing, 41, 1062-1074, 2003.

Guo, Z., Liu, T., Guiot, J., Wu, N., Lv, H., Han, J., Liu, J., and Gu, Z.: High frequency pulses of East Asian monsoon climate in the last two glaciations: link with the North Atlantic, Clim. Dynam., 12, 701–709, 1996.

Halley, E.: An historical account of the trade winds and monsoons observable in the seas between and near the tropics with an attempt to assign the physical cause of the said wind, Philos. T. R. Soc. Lond., 16, 153–168, 1986.

Heinrich, H.: Origin and consequences of cyclic ice rafting in the Northeast Atlantic Ocean during the past 130,000 years, Quaternary Res., 29, 142–152, 1988.

Hu, C., Henderson, G. M., Huang, J., Xie, S., Sun, Y., and Johnson, K. R.: Quantification of Holocene Asian monsoon rainfall from spatially separated cave records, Earth Planet. Sc. Lett., 266, 221–232, 2008.

Hu, Z. and Wu, Z.: The intensification and shift of the annual North Atlantic Oscillation in a global warming scenario simulation, Tellus, 56, 112-124, 2004.

Huang, N. E., Shen, Z., Long, S. R., Wu, M. C., Shih, H. H., Zheng, Q., Yen, N. C., Tung, C. C., and Liu, H. H.: The empirical mode decomposition and the Hilbert spectrum for nonlinear and non-stationary time series analysis, The Royal Society, 454, 903-995, 1998.

Jin, L., Chen, F., Ganopolski, A., and Claussen, M.: Response of East Asian climate to Dansgaard/Oeschger and Heinrich events in a coupled model of intermediate complexity, J. Geophys. Res., 112, D06117, doi:10.1029/2006JD007316, 2007.

Kelly, M. J., Edwards, R. L., Cheng, H., Yuan, D., Cai, Y., Zhang, M., Lin, Y., and An, Z.: High resolution characterization of the Asian Monsoon between 146,000 and 99,000 years B. P. from Dongge Cave and global correlation of events surrounding Termination II, Palaeogeogr. Palaeocl., 236, 20–38, 2006.

Lestari, R. and Iwasaki, T.: A GCM study on the roles of the seasonal marches of the SST and land–sea thermal contrast in the onset of the Asian summer monsoon, J. Meteorol. Soc. Jpn., 84, 69–83, 2006.

Lin, Z. and Wang, S.: EMD analysis of solar insolation, Meteorol. Atoms. Phys., 93, 123-128, 2006.

Lisiecki, L. E. and Raymo, M. E.: A Pliocene-Pleistocene stack of 57 globally distributed benthic $\delta^{18}O$ records, Paleoceanography, 20, PA1003, doi:10.1029/2004PA001071, 2005.

Liu, T. and Ding, Z.: Chinese loess and the paleomonsoon, Annu. Rev. Earth Pl. Sc., 26, 111– 145, 1998.

Liu, T., Ding, Z., and Rutter, N.: Comparison of Milankovitch periods between continental loess and deep sea records over the last 2.5 Ma, Quaternary Sci. Rev., 18, 1205–1212, 1999.

Liu, Z., Wen, X., Brady, E. C., Otto-Bliesner, B., Yu, G., Lu, H., Cheng, H., Wang, Y., Zheng, W., Ding, Y., Edwards, R. L., Cheng, J., Liu, W., and Yang, H.: Chinese cave records and the East Asian Summer Monsoon, Quaternary Sci. Rev., 83, 115-128, 2014.

Lu, H., Huissteden, K. V., An, Z., Nugteren, G., and Vandenberghe, J.: East Asia winter monsoon variations on a millennial time-scale before the last glacial–interglacial cycle, J. Quaternary Sci., 14, 101–110, 1999.

Lu, H., Yi, S., Liu, Z., Mason, J. A., Jiang, D., Cheng, J., Stevens, T., Xu, Z., Zhang, E., Jin, L., Zhang, Z., Guo, Z., Wang, Y., and Otto-Bliesner, B.: Variation of East Asian monsoon precipitation during the past 21 k.y., and potential CO_2 forcing, Geology, 41, 1023–1026, 2013.

Lu, H., Zhang, F., and Liu, X.: Patterns and frequencies of the East Asian winter monsoon variations during the past million years revealed by wavelet and spectral analyses, Global Planet. Change, 35, 67–74, 2003.

Maher, B. A. and Thompson, R.: Oxygen isotopes from Chinese caves: records not of monsoon rainfall but of circulation regime, J. Quaternary Sci., 27, 615–624, 2012.

McManus, J. F., Oppo, D. W., and Cullen, J. L.: A 0.5-million-year record of millennial-scale climate variability in the North Atlantic, Science, 283, 971–975, 1999.

Meese, D. A., Gow, A. J., Alley, R. B., Zielinski, G. A., Grootes, P. M., Ram, M., Taylor, K. C., Mayewski, P. A., and Blozan, J. F.: The Greenland Ice Sheet Project 2 depth-age scale:

methods and results, J. Geophys. Res., 102, 26411–26423, 1997.

Miao, X., Sun, Y., Lu, H., and Mason, J. A.: Spatial pattern of grain size in the Late Pliocene "Red Clay" deposits (North China) indicates transport by low-level northerly winds, Palaeogeogr. Palaeocl., 206, 149–155, 2004.

Molla, K., Sumi, A., and Rahman, M.: Analysis of temperature change under global warming impact using Empirical Mode Decomposition, Int. J. Information Technol., 3, 131-139, 2006.

Palmer, T. N. and Sun, Z.: A modelling and observational study of the relationship between sea surface temperature in the North-West Atlantic and the atmospheric general circulation, Q. J. Roy. Meteor. Soc., 111, 947–975, 1985.

Pausata, F. S. R., Battisti, D. S., Nisancioglu, K. H., and Bitz, C. M.: Chinese stalagmite $\delta^{18}O$ controlled by changes in the Indian monsoon during a simulated Heinrich event, Nat. Geosci., 4, 474–480, 2011.

Peterse, F., Prins, M. A., Beets, C. J., Troelstra, S. R., Zheng, H., Gu, Z., Schouten. S., and Damsté, J. S. S.: Decoupled warming and monsoon precipitation in East Asia over the last deglaciation, Earth Planet. Sc. Lett., 301, 256–264, 2011.

Porter, S. C. and An, Z.: Correlation between climate events in the North Atlantic and China during the last glaciation, Nature, 375, 305–308, 1995.

Rodwell, M. J., Rowell, D. P., and Folland, C. K.: Oceanic forcing of the wintertime North Atlantic Oscillation and European climate, Nature, 398, 320–323, 1999.

Schulz, M. and Mudelsee, M.: REDFIT: estimating red-noise spectra directly from unevenly spaced paleoclimatic time series, Comput. Geosci., 28, 421–426, 2002.

Schulz, M. and Stattegger, K.: Spectrum: spectral analysis of unevenly spaced palaeoclimatic time series, Comput. Geosci., 23, 929-945, 1997.

Shi, Z., Liu, X., Sun, Y., An, Z., Liu, Z., and Kutzbach, J.: Distinct responses of East Asian summer and winter monsoons to astronomical forcing, Clim. Past, 7, 1363–1370, 2011.

Sun, Y., Clemens, S. C., An, Z., and Yu, Z.: Astronomical timescale and palaeoclimatic implication of stacked 3.6-Myr monsoon records from the Chinese Loess Plateau, Quaternary

Sci. Rev., 25, 33–48, 2006.

Sun, Y., Clemens, S. C., Morrill, C., Lin, X., Wang, X., and An, Z.: Influence of Atlantic meridional overturning circulation on the East Asian winter monsoon, Nat. Geosci., 5, 46–49, 2012.

Sun, Y., Kutzbach, J., An, Z., Clemens, S., Liu, Z., Liu, W., Liu, X., Shi, Z., Zheng, W., Liang, L., Yan, Y., and Li, Y.: Astronomical and glacial forcing of East Asian summer monsoon variability, Quaternary Sci. Rev., 115, 132-142, 2015.

Sun, Y., Wang, X., Liu, Q., and Clemens, S. C.: Impacts of post-depositional processes on rapid monsoon signals recorded by the last glacial loess deposits of northern China, Earth Planet. Sc. Lett., 289, 171–179, 2010.

Vautard, R., Yiou, P., and Ghil, M.: Singular-spectrum analysis: a toolkit for short, noisy chaotic signals, Physica D: Nonlinear Phenomena, 58, 95-126, 1992.

Wang, L., Sarnthein, M., Erlenkeuser, H., Grimalt, J., Grootes, P., Heilig, S., Ivanova, E., Kienast, M., Pelejero, C., Pflaumaan, U.: East Asian monsoon climate during the Late Pleistocene: high-resolution sediment records from the South China Sea, Mar. Geol., 156, 245–284, 1999.

Wang, P., Clemens, S., Beaufort, L., Braconnot, P., Ganssen, G., Jian, Z., Kershaw, P., Sarnthein, M.: Evolution and variability of the Asian monsoon system: state of the art and outstanding issues, Quaternary Sci. Rev., 24, 595-629, 2005.

Wang, Y., Cheng, H., Edwards, R. L., An, Z., Wu, J., Shen, C., and Dorale, J. A.: A high resolution absolute-dated late Pleistocene monsoon record from Hulu Cave, China, Science, 294, 2345–2348, 2001.

Wang, Y., Cheng, H., Edwards, R.L., Kong, X., Shao, X., Chen, S., Wu, J., Jiang, X., Wang, X., and An, Z.: Millennial and orbital-scale changes in the East Asian monsoon over the past 224,000 years, Nature, 451, 1090–1093, 2008.

Xiao, J., Porter, S. C., An, Z., Kumai, H., and Yoshikawa, S.: Grain size of quartz as an indicator of winter monsoon strength on the Loess Plateau of central China during the last

130,000 yr, Quaternary Res., 43, 22–29, 1995.

Yang, S. and Ding, Z.: A 249 kyr stack of eight loess grain size records from northern China documenting millennial-scale climate variability, Geochem. Geophy. Geosy., 15, 798–814, 2014.

Yang, Z., Lin, Z., and Yu, M.: Multi-scale analysis of East Asian winter monsoon evolution and Asian inland drying force (in Chinese), Quaternary Sci., 31, 73–80, 2011.

Yang, Z., Lin, Z., Yu, M., Zhang, Z.: Significant multi-scale analysis on evolution of the East Asian summer monsoon on the Loess Plateau during the last 1 MaB.P. (in Chinese), Geography and Geo-information Science, 24, 93-97, 2008.

Yuan, D., Cheng, H., Edwards, R. L., Dykoski, C. A., Kelly, M. J., Zhang, M., Qing, J., Lin, Y., Wang, Y., Wu, J., Dorale, J. A., An, Z., and Cai, Y.: Timing, duration, and transitions of the last interglacial Asian monsoon, Science, 304, 575–578, 2004.

Zhang, R. and Delworth, T. L.: Simulated tropical response to a substantial weakening of the Atlantic thermohaline circulation, J. Climate, 18, 1853–1860, 2005.

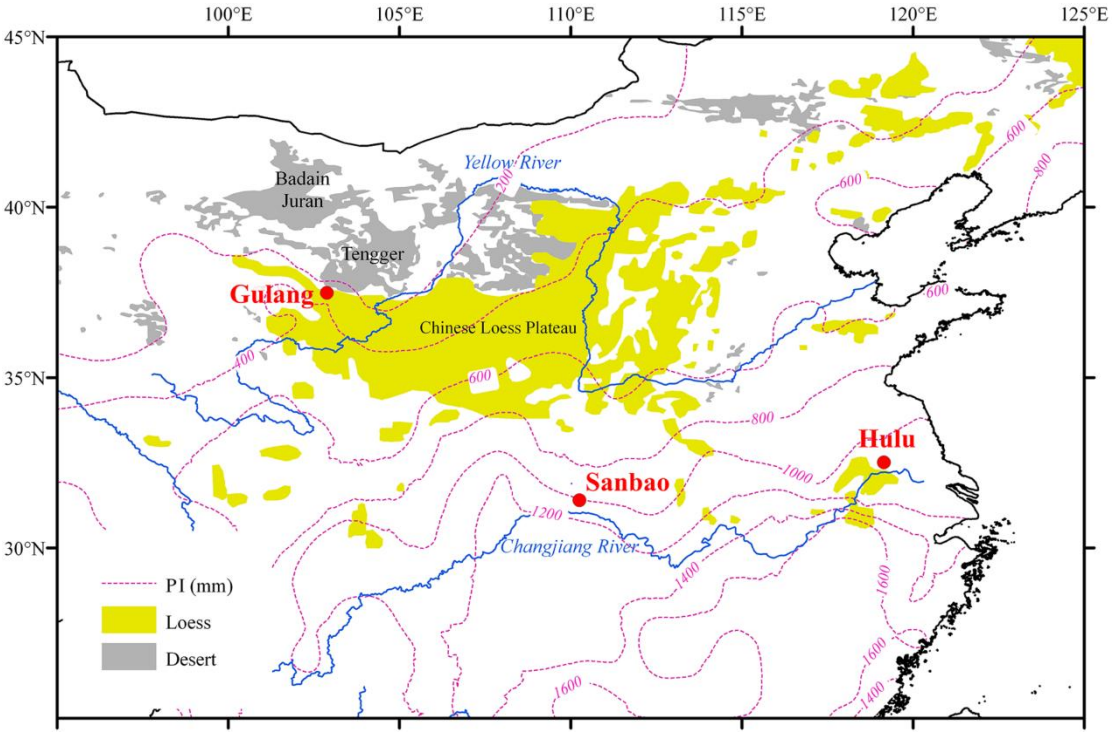

Figure 1. Map showing the loess distribution and locations of Gulang loess section, Sanbao, and Hulu caves. Dotted lines indicate the precipitation isohyets (PI).

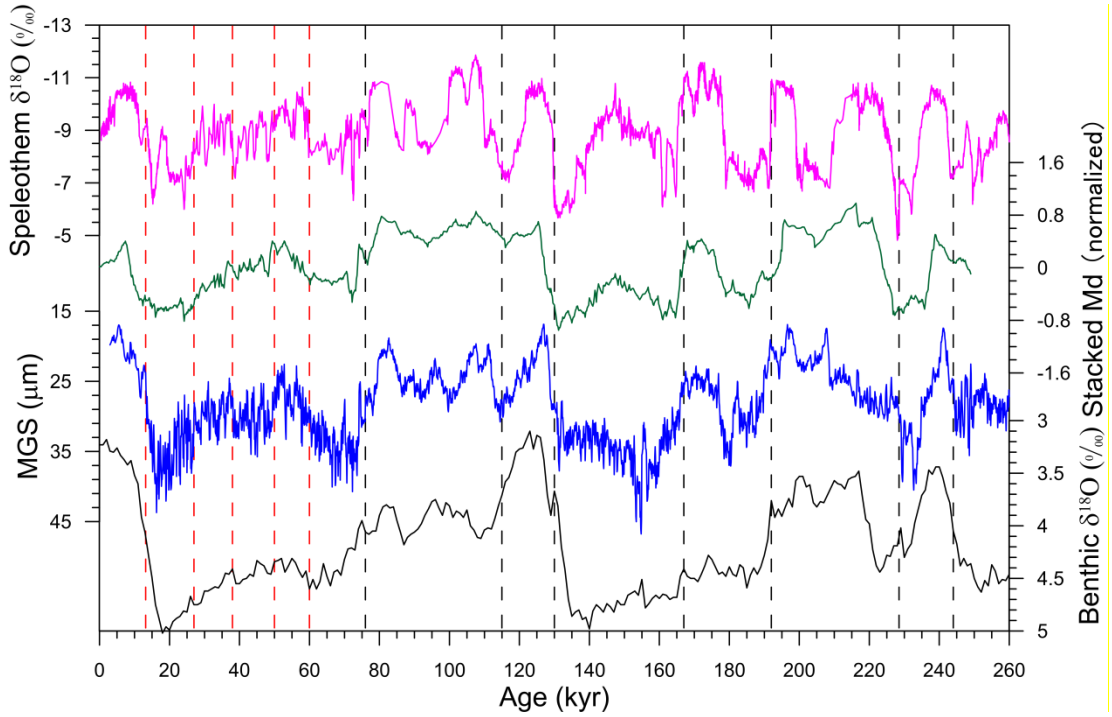

Figure 2. Comparison of Gulang MGS (blue) and CHILOMOS stack Median grain size (Md, green, Yang and Ding, 2014) with the benthic $\delta^{18}O$ (black, Isiecki and Raymo, 2005) and Sanbao/Hulu speleothem $\delta^{18}O$ (magenta, Wang et al., 2008; Cheng et al., 2009) records. The red and black dashed lines denote tie points derived from OSL dating and benthic $\delta^{18}O$ correlation, respectively.

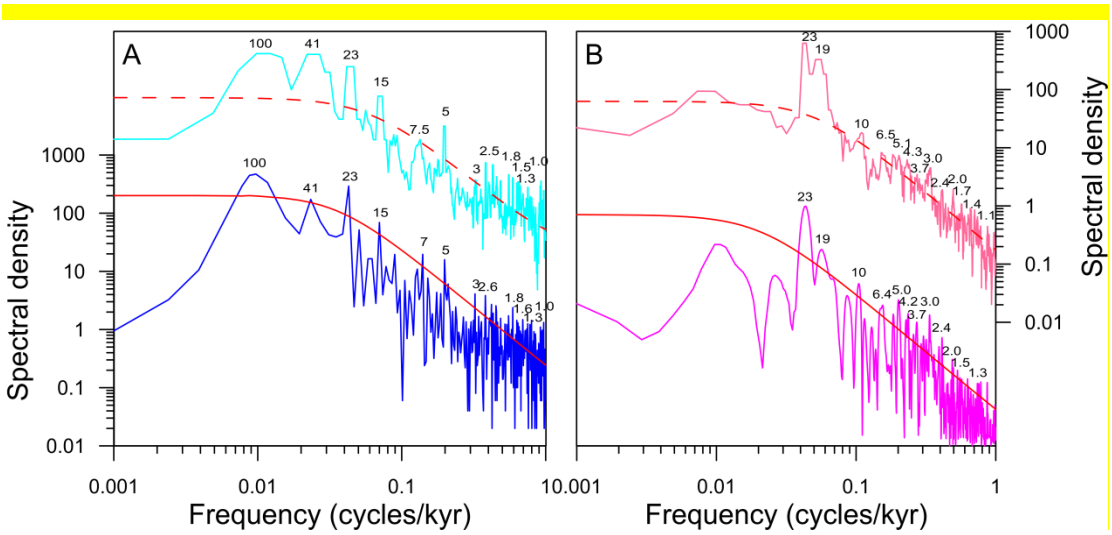

Figure 3. Spectrum results of Gulang MGS (A) and Sanbao/Hulu speleothem $\delta^{18}O$ (B) (Wang et al., 2008; Cheng et al., 2009) records using REDFIT (lower) and MTM (higher) methods. The red lines represent the 80% (solid) and 90% (dotted) confidence levels. Periodicities are shown above the spectral curves.

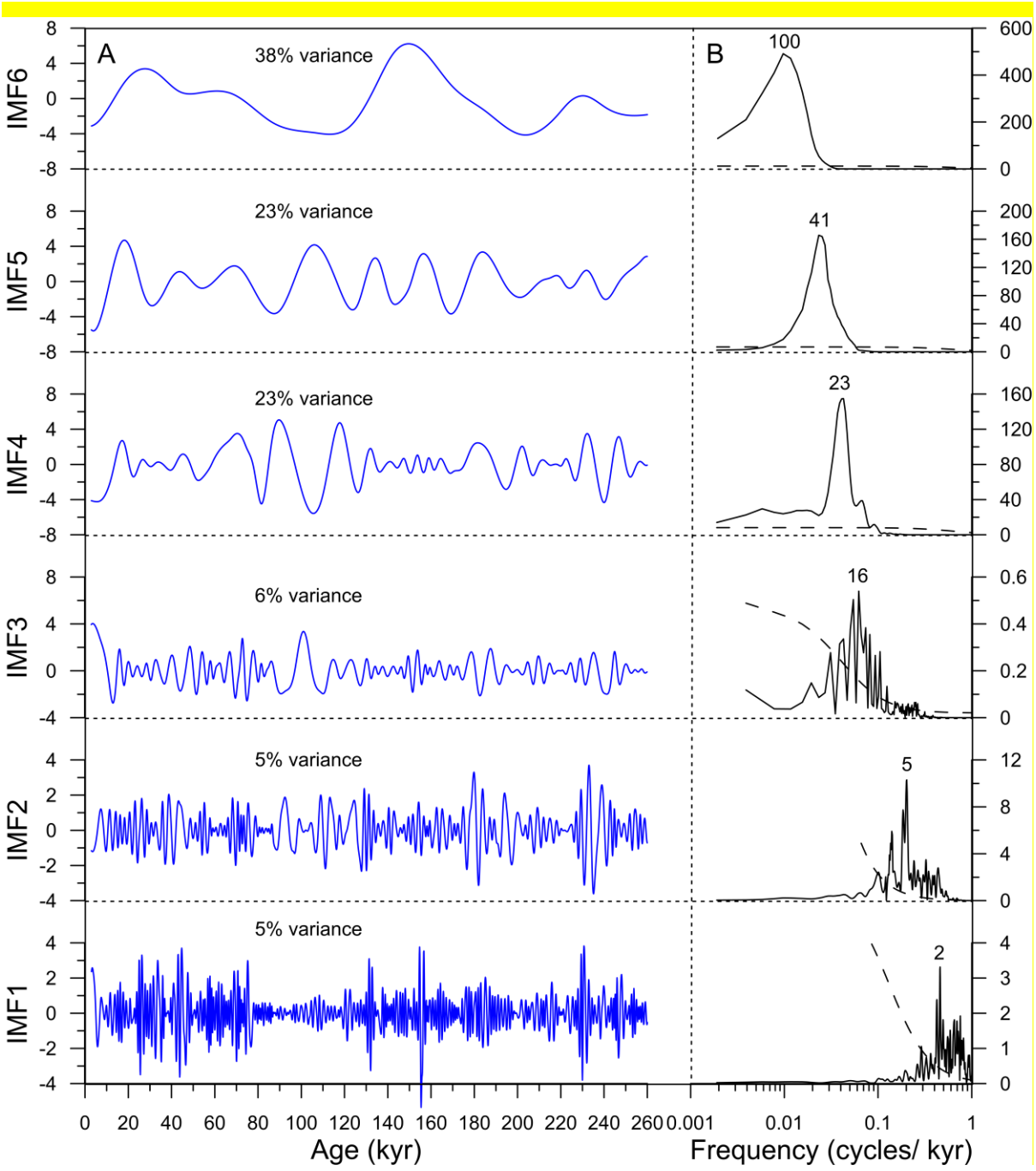

Figure 4. IMFs of Gulang MGS series (A) and corresponding spectrum (B). Black numbers are dominant periods and dotted lines represent the 90% confidence level.

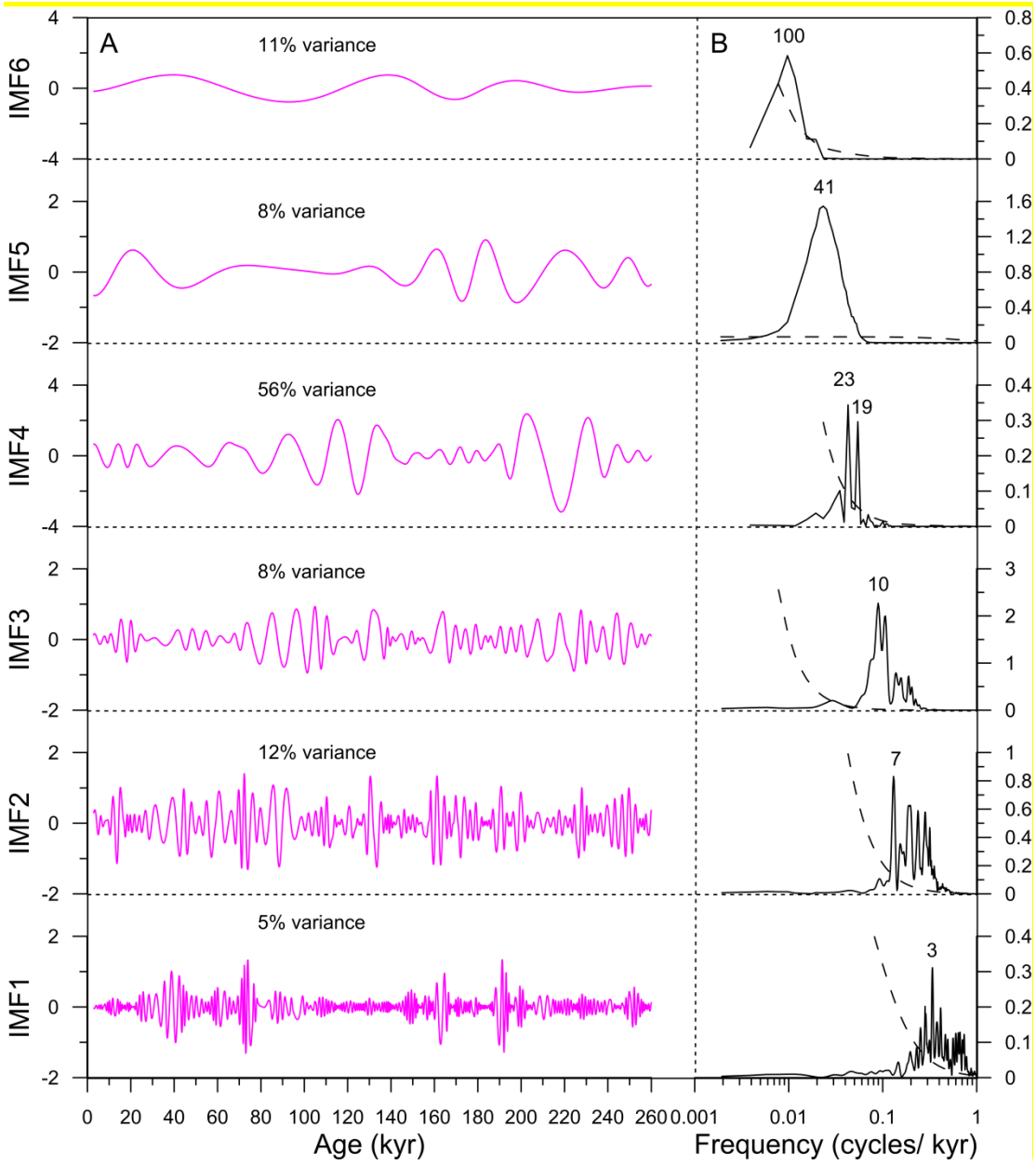

Figure 5. IMFs of speleothem $\delta^{18}O$ series (A) and corresponding spectrum (B). Black numbers are dominant periods and dotted lines represent the 90% confidence level.

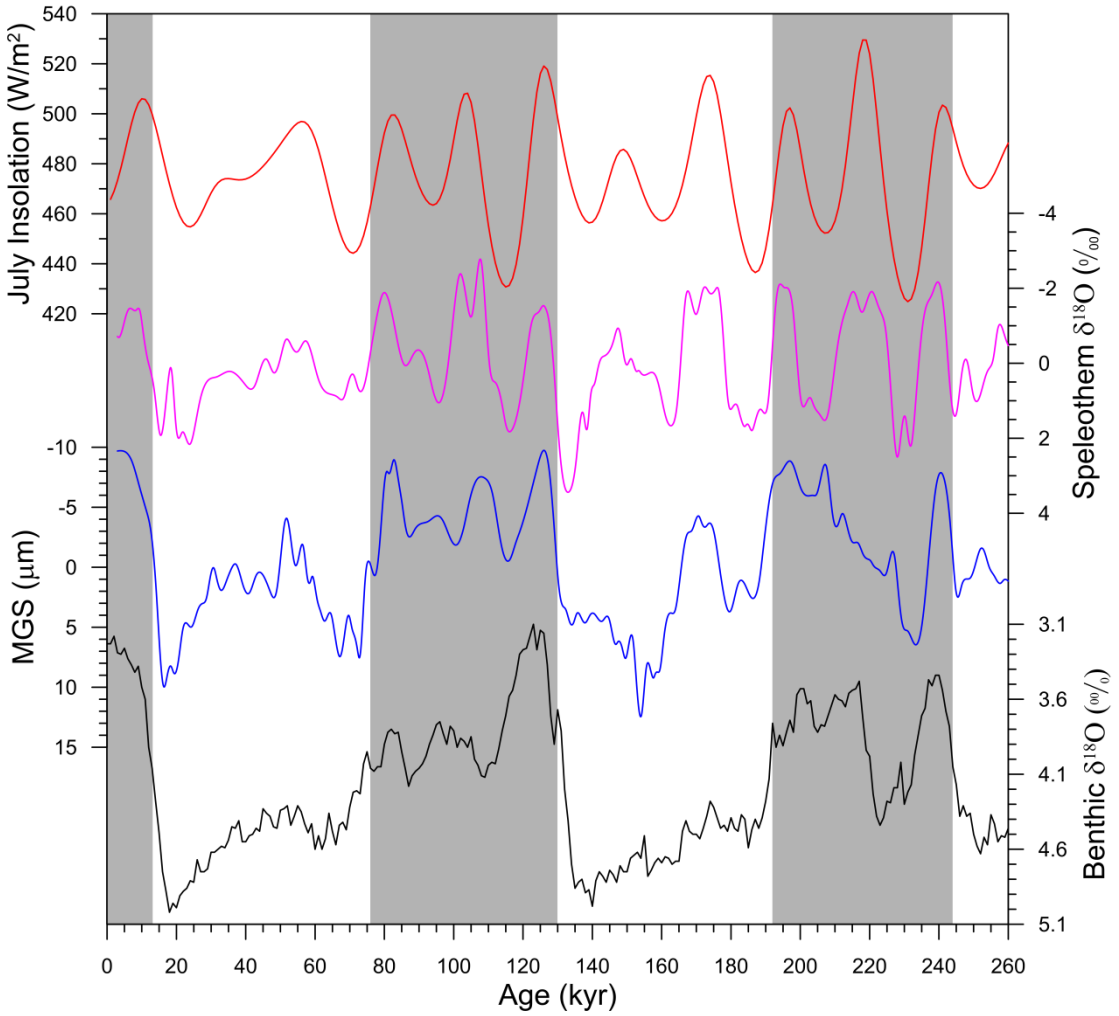

Figure 6. Comparison of the glacial-and-orbital scale components of Gulang MGS (blue) and Sanbao/Hulu speleothem $\delta^{18}O$ (magenta, Wang et al., 2008; Cheng et al., 2009) records with summer insolation at 65 ºN (red, Berger, 1978) and benthic $\delta^{18}O$ record (black, Lisiecki and Raymo, 2005). The vertical gray bars represent the interglacial periods.

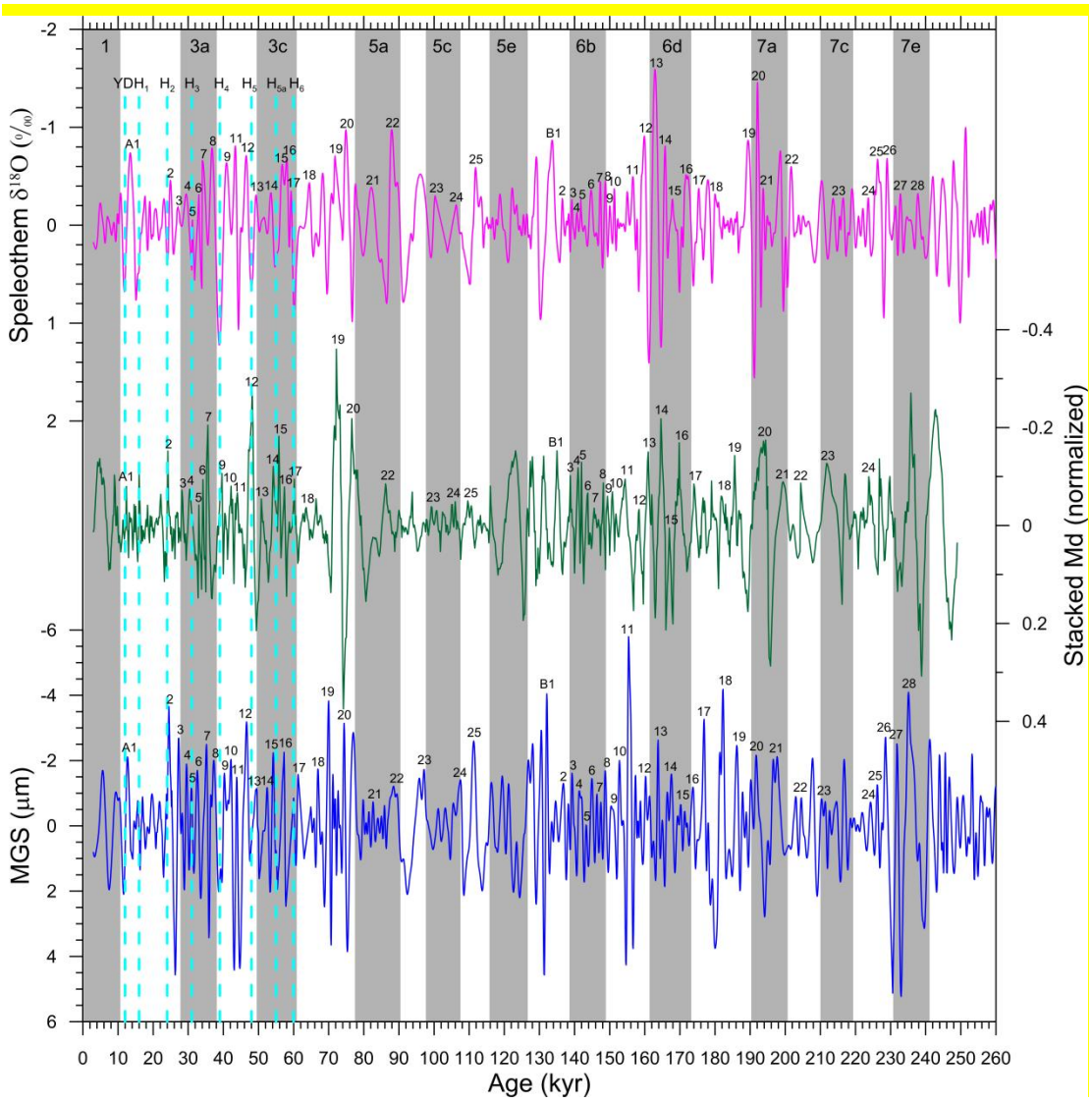

Figure 7. Comparison of millennial-scale variations among Gulang MGS (blue), CHILOMOS stack Md (green, Yang and Ding, 2014) and Sanbao/Hulu speleothem $\delta^{18}O$ (magenta, Wang et al., 2008; Cheng et al., 2009) records over the last two glacial–interglacial cycles. Cyan dotted lines are the YD and the Heinrich events recorded in the three records and gray bars indicate interglacial periods. The numbers represent well-correlated Chinese interstadials identified among the three records.